PHILOSOPHICAL TRANSACTIONS OF THE ROYAL SOCIETY A MATHEMATICAL, PHYSICAL & ENGINEERING SCIENCES

The Band Structure and Fermi Surface of Magnesium

L. M. Falicov

Phil. Trans. R. Soc. Lond. A 1962 **255**, 55-83
doi: 10.1098/rsta.1962.0010

THE BAND STRUCTURE AND FERMI SURFACE OF MAGNESIUM

By L. M. FALICOV†

Cavendish Laboratory, University of Cambridge

(*Communicated by A. B. Pippard, F.R.S.—Received* 16 *February* 1962)

CONTENTS

A calculation of the band structure of magnesium metal is performed by means of the orthogonalized plane wave method, in a similar way to that done by Heine for aluminium. The various contributions to the lattice potential are carefully analyzed and computed in order to obtain a final accuracy of about 0·035 Ry, including the errors due to convergence of the secular equation. Group-theory methods are used to evaluate the energy levels at points of symmetry and to test the accuracy of the numerical methods. The Fermi energy is obtained by comparison with the free-electron model. The Fermi surface is then described with emphasis on its geometrical and topographical properties to allow for direct comparison with experiment.

1. Introduction

The rapid development in the last 5 years of several experimental techniques, such as the de Haas–van Alpen effect and cyclotron resonance, which yield accurate information on the properties of the electronic structure of metals, has produced a revival of the calculation of detailed band structures in terms of which experimental data could be interpreted. On the other hand, the increasing understanding of the behaviour of electrons in a metal, mainly the effects of electron-electron interactions, allows a better determination of the effective potential acting on the conduction electrons and consequently the possibility of computing accurate band structures using some of the well-known numerical techniques (Reitz 1955; Herman 1958). In this context magnesium stands as a very interesting and promising metal. The number of core electrons is fairly low and good determinations of the Hartree–Fock function of the Mg^{2+} ion (Jacque-Yost 1940) and atomic Mg (Biermann & Trefftz 1949) are available; its position in the periodic table is adjacent to Na (Cohen & Heine 1958) and Al (Heine 1957), metals that are known to be free-electron-like and for which the orthogonalized-plane-wave (*OPW*) method is rapidly convergent. In addition, several experiments for determining properties of the Fermi surface of magnesium (Priestley, to be published; Shoenberg 1960; Fawcett 1961; Gordon, Joseph & Eck 1960) were under way when the present calculation was started, and a fairly accurate theoretical model was necessary in order to have a solid standpoint for the interpretation of the experimental information.

† Present address: Institute for the Study of Metals, University of Chicago, Chicago 37, Illinois.

Vol. 255. A. 1051. (Price 9*s*.) 8 [Published 25 October 1962

This paper describes the procedure and results of a band structure calculation for magnesium metal, by the use of the *OPW* method (Heine 1957; Woodruff 1957). The various contributions to the crystal potential acting on the conduction electrons are discussed in § 2. They are divided into eleven items which are computed in turn together with an estimate of their contributions to the final error. Section 3 is concerned with the *OPW*s, the determination of their coefficients, the setting down of the secular equations for the band energies and their numerical solution. Section 4 is devoted to the study of the symmetry properties of the lattice. They have been used to factorize the secular equation and to obtain the band energy of the symmetry points with greater accuracy. These points are used to check the convergence of the method and to determine the errors due to the truncation of the secular equation. The accuracy of the complete scheme and the final errors in the band energies are discussed in § 5. Finally, the estimation of the Fermi energy and the shape and dimensions of the Fermi surface are described in § 6, as well as some of its topological properties.

2. The lattice potential

The units used throughout this paper are such that $m = \hbar = e = 1$. With this choice the unit of length turns out to be the Bohr radius a_0. The energy is expressed in rydbergs (Ry);

$$a_0 = 0{\cdot}529\ \text{Å},$$
$$1\text{Ry} = 13{\cdot}6\ \text{eV}.$$

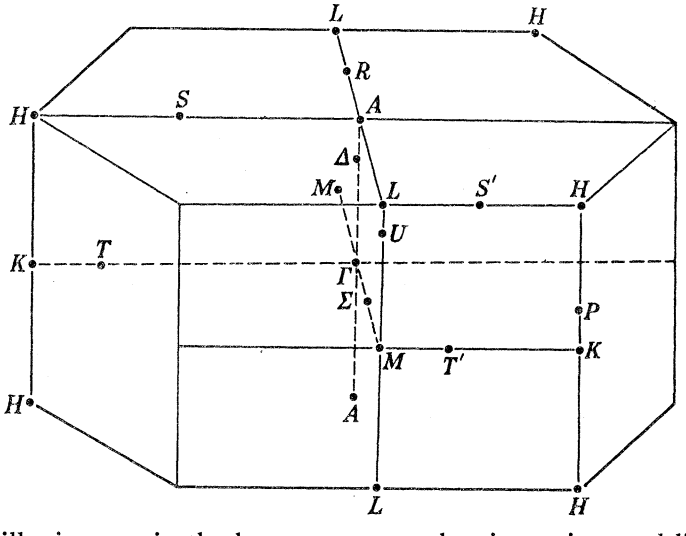

Figure 1. The Brillouin zone in the h.c.p. structure showing points and lines of symmetry. The size of the zone is given in table 3.

Magnesium crystallizes in a close-packed hexagonal structure (h.c.p.) whose lattice constants, extrapolated to 0 °K are

$$a = 3{\cdot}189\ \text{Å} = 6{\cdot}026\, a_0,$$
$$c = 5{\cdot}177\ \text{Å} = 9{\cdot}784\, a_0.$$

The ratio $c/a = 1{\cdot}624$ is very near to the perfect packing ratio 1·633. The properties of the direct and reciprocal lattices are given in tables 1 and 2, respectively. The reduced Brillouin zone (Herring 1942; Antoncik & Triflaj 1952; Altmann 1958) is shown in figure 1 and the co-ordinates of the symmetry points, following Herring's notation (1942), are given in table 3.

TABLE 1. THE MAGNESIUM H.C.P. DIRECT LATTICE

	x	y	z
$\mathbf{t}_1$	0	0	9·784
$\mathbf{t}_2$	6·026	0	0
$\mathbf{t}_3$	−3·013	5·219	0
$(\mathbf{t}_4)$	−3·013	−5·219	0

unit cell volume	307·68
atomic volume Ω_0	153·84
atomic radius r_0	3·324

TABLE 2. THE MAGNESIUM RECIPROCAL LATTICE

	x	y	z
$\mathbf{G}_1$	0	0	0·6422
$\mathbf{G}_2$	1·0426	0·6020	0
$\mathbf{G}_3$	0	1·2040	0
$(\mathbf{G}_4)$	−1·0426	0·6020	0

$\mathbf{G}_i.\mathbf{t}_j = 2\pi\delta_{ij} \quad (i, j = 1, 2, 3)$

volume of the Brillouin zone	0·8062
volume of occupied states	1·6124
radius of the free electron distribution (Fermi momentum)	0·7274

TABLE 3. SYMMETRY POINTS OF THE MAGNESIUM BRILLOUIN ZONE

	orthogonal co-ordinates			reciprocal lattice			magnitude
point	x	y	z	G_2	G_3	G_1	k
Γ	0	0	0	0	0	0	0
A	0	0	0·3211	0	0	$\frac{1}{2}$	0·3211
M	0·5213	0·3010	0	$\frac{1}{2}$	0	0	0·6020
L	0·5213	0·3010	0·3211	$\frac{1}{2}$	0	$\frac{1}{2}$	0·6823
K	0·6951	0	0	$\frac{2}{3}$	$-\frac{1}{3}$	0	0·6951
K'	0·3475	0·6020	0	$\frac{1}{3}$	$\frac{1}{3}$	0	0·6951
H	0·6951	0	0·3211	$\frac{2}{3}$	$-\frac{1}{3}$	$\frac{1}{2}$	0·7657
H'	0·3475	0·6020	0·3211	$\frac{1}{3}$	$\frac{1}{3}$	$\frac{1}{2}$	0·7657

As it has been pointed out repeatedly, the main source of errors in any band-structure calculation is the uncertainty that exists in determining the net potential acting on an electron moving through the lattice. This uncertainty gave rise, before Heine's calculation (1957), to errors in the band energies of the order of 0·2 Ry. The detailed calculation of the band structure of aluminium done by Heine was the first successful attempt to decrease this error, reducing it to the order of 0·03 Ry. In the last 5 years extensive studies on the many-body properties of the electron gas have shown that the one-electron approximation is justified, at least near the Fermi surface. This result eliminates the main source of conceptual uncertainty in the setting up of the lattice potential, i.e. the correlation and exchange terms. Apart from such conceptual problems, errors arise as a result of difficulties in the computation, e.g. the necessity to assume spherically symmetrical potentials around each nucleus. In any case, by considering and analyzing every contribution we attempt to get a final error of the order of that obtained by Heine for aluminium. Near the Fermi surface, where the one-electron approximation strictly holds, our results must be more accurate and physically reliable; the experimental information will be the final criterion to estimate the accuracy of the present calculation.

Following Heine (1957) we enumerate the various contributions to the potential:

(*a*) potential due to the ion-core,
(*b*) exchange among ion-core electrons,
(*c*) correlation among ion-core electrons,
(*d*) exchange between conduction and core electrons,
(*e*) correlation between conduction and core electrons,
(*f*) potential due to the conduction electrons,
(*g*) the deviation from spherical symmetry around the core,
(*h*) exchange among conduction electrons,
(*i*) correlation among conduction electrons,
(*j*) spin-orbit coupling,
(*k*) self consistency and remaining errors of the whole scheme.

The main contributions come from (*a*) and (*f*); (*b*) (*d*), (*h*) and (*i*) give important corrections; (*c*) and (*g*) give second-order corrections; (*j*) is negligible in magnitude but introduces important changes in the topology of the energy surfaces; (*e*) is negligible for magnesium. If (*a*) to (*j*) have been computed correctly, (*k*) will in general be negligible.

The total potential is expressed as a sum of identical atomic-like potentials centred at each ion

$$V(\mathbf{r}) = \sum_{\alpha} U(|\mathbf{r}-\mathbf{R}_{\alpha}|), \tag{2·1}$$

$$U(r) = -(2/r)\, Z_P(r), \tag{2·2}$$

where for magnesium Z_P must satisfy the two conditions

$$Z_P(0) = 12, \quad Z_P(\infty) = 0. \tag{2·3}$$

The magnesium core electrons 1*s*, 2*s* and 2*p* are tightly bound electrons and their atomic wave functions, except for phase factors, are not fundamentally disturbed by the presence of the lattice or the conduction electrons. This means that their crystal wave functions can be adequately represented by Bloch tight-binding orbitals. Consequently the potential acting on conduction electrons due to the core, except for exchange and correlation effects, is the potential seen by a test charge in the neighbourhood of a Mg^{2+} ion. To compute this potential it is necessary to know the electronic wave functions of Mg^{2+} and to solve Poisson's equation for the distribution of charge given by them. These are the standard techniques used for calculating atomic structures with self-consistent fields (Hartree 1957) and have been applied to the already computed radial functions of Mg^{2+} (Jacque-Yost 1940) to obtain the contribution $2Z_1$ to $2Z_P$ (the total potential) shown in table 4. The numerical integration of the Poisson equation was performed on EDSAC 2, the computer of the University of Cambridge Mathematical Laboratory, by the use of available standard routines.

Correlation among the ion-core electrons is a second-order correction and a rather unimportant one. It can be computed by expanding the Mg^{2+} electronic wave function in series of determinants instead of using a single Slater determinant. No detailed calculation of this sort is available for Mg^{2+}, but it has been performed for Na^{+} (Bernal & Boys 1952). Heine (1957) has compared the corresponding charge distribution with that obtained

TABLE 4. THE LATTICE POTENTIAL

r	$2Z_1$	$2Z_2$	$2Z_3$	$2Z_4$	$2Z_5$	$2Z_P$
0	24·000	0·000	0·000	0·000	0·000	24·000
0·025	22·099	−0·004	0·387	−0·045	0·005	22·442
0·05	20·417	−0·007	0·693	−0·090	0·009	21·022
0·10	17·780	−0·014	1·118	−0·181	0·019	18·723
0·15	15·809	−0·021	1·746	−0·271	0·028	17·292
0·20	14·188	−0·028	0·180	−0·361	0·038	14·017
0·28	11·993	−0·039	1·040	−0·504	0·053	12·542
0·36	10·160	−0·048	1·338	−0·647	0·068	10·870
0·44	8·661	−0·052	1·586	−0·798	0·083	9·488
0·52	7·472	−0·053	1·824	−0·931	0·098	8·409
0·60	6·555	−0·053	2·111	−1·001	0·113	7·654
0·80	5·144	−0·043	3·554	−1·484	0·150	7·389
1·00	4·495	−0·029	−2·026	−1·751	0·188	0·876
1·20	4·211	−0·016	−0·262	−2·072	0·225	2·086
1·60	4·039	−0·004	0·016	−2·665	0·300	1·686
2·00	4·008	−0·001	0·018	−3·175	0·375	1·226
2·60	4·001	0·000	0·006	−3·736	0·443	0·713
3·40	4·000	0·000	0·001	−4·000	0·217	0·218
4·20	4·000	0·000	0·000	−4·000	0·005	0·005
5·00	4·000	0·000	0·000	−4·000	0·000	0·000

Note. The lattice potential is expressed in the form (2·2).

r the radius in atomic units.
$2Z_1$ potential due to the ion-core.
$2Z_2$ correlation among ion-core electrons.
$2Z_3$ exchange between core and conduction electrons.
$2Z_4$ potential due to conduction electrons.
$2Z_5$ potential due to the deviation from uniform distribution of conduction electrons around each nucleus.
$2Z_P$ the total potential excluding correlation and exchange among conduction electrons.

using the Hartree–Fock approximation in Na^+ (Hartree & Hartree 1948) and has calculated the potential due to the difference. This is listed as $2Z_2$ in table 4. As expected, correlation effects allow the electrons to pack into a smaller volume. The contribution to $2Z_P$, although very small, is then negative. The correction due to the difference in atomic number between Na^+ and Mg^{2+} is neglected, being unimportant in such a small term. The errors involved in the potential due to the ion-core electrons (items (*a*) to (*c*)) are orders of magnitude smaller than the proposed final error, so that no significant error contribution arises from them.

We now consider the contribution to the potential due to exchange between conduction and core electrons. If we restrict ourselves to some points of high symmetry in the Brillouin zone, the wave functions of the conduction electrons have a definite symmetry around each nucleus, i.e. they behave approximately as an atomic wave function of definite angular symmetry. For instance, the *s*-like functions behave essentially like atomic 3*s*-functions, except for an amplitude factor. The exchange of such a function with the ion-core electrons, only important in the ion-core region, is substantially the same as the exchange involving the Mg atom 3*s*-function. Using again the well-known methods for computing exchange in atomic structures, we find that the contribution of the 3*s*-function to the exchange part of the Hamiltonian is given by

$$Y_{3s}(x) = 2\sum_t \psi_t(x) \int \psi_t^*(y)\, \psi_{3s}(y)\, \frac{1}{r_{xy}}\, \mathrm{d}^3y, \qquad (2{\cdot}4)$$

$$t = 1s, 2s, 2p_x, 2p_y, 2p_z.$$

We express this term as an effective potential $U_{3s}^{\text{ex.}}$.

$$Y_{3s}(x) = U_{3s}^{\text{ex.}}(x)\,\psi_{3s}(x) \tag{2·5}$$

and in turn, using the radial symmetry of the system, we have

$$U_{3s}^{\text{ex.}} = -2Z_3(r)/r. \tag{2·6}$$

$Y_{3s}(x)$ and $2Z_3(r)$ have been computed by the use of the techniques described by Hartree (1957), which amount to the solution of a system of differential equations with tabulated coefficients and known boundary conditions. The functions involved in the calculation are the Mg^{2+} 1*s*-, 2*s*-, and 2*p*-functions (Jacque-Yost 1940) and the Mg atom 3*s*-function (Biermann & Trefftz 1949) already available in the literature. The result $2Z_3(r)$ is shown in table 4. Equations similar to (2·4), (2·5) and (2·6) exist for 3*p*-electrons. It is worth noting that the exchange potential as expressed by (2·5) is independent of the amplitude of ψ_{3s} and is equally valid to a very good approximation for the atomic 3*s*-function and the lowest *s*-like crystal orbitals of the metal.

Heine has calculated the effective exchange potential for the 3*s*- and 3*p*-orbitals in aluminium and has shown that both are very nearly the same over the range where exchange is important. The error in the energies due to using the *s*-potential for a *p*-like function is less than 0·01 Ry. In Mg most of the conduction band actually occupied by electrons is *s*-like or has *s*-like contributions; so we have chosen the 3*s* exchange potential to represent the exchange potential of the whole band. The error involved in this approximation is less than 0·01 Ry for *p*-like states or states of higher angular symmetry around the nuclei, and much less for the rest of the band.

The rather large oscillations of $2Z_3$ near $r = 0{\cdot}18$ and $r = 0{\cdot}90$ are due to the fact that the exchange term (2·4) does not vanish at the nodes of the radial 3*s*-function, so that $2Z_3$ tends to $\pm\infty$ near these points. The potential $U_{3s}^{\text{ex.}}$ has been smoothed out over a small range of r near the nodes of the radial 3*s*-function. The error caused by this approximation is negligible because the 3*s*-functions are very small (approximately zero) at those values.

Exchange between the conduction electrons and the various core electrons (item (*d*) of the potential) is an additive effect as shown by (2·5). On the other hand, correlation effects (item (*e*)) have a very complicated dependence and are difficult to compute. They have been completely neglected in the present calculation. To estimate the error involved in this approximation a perturbation calculation has been performed once the band structure and the crystal wave functions were known, with the use as a perturbation potential of the contribution of correlation to the separation energy considered as a function of the local density. The correlation energy per particle ϵ_c is generally expressed in terms of the parameter

$$r_s \equiv (3/4\pi n)^{\frac{1}{3}}, \tag{2·7}$$

where n is the density of electrons in atomic units. The function $\epsilon_c(r_s)$ has different expressions for the various density ranges. In the high density limit ($r_s \leqslant 1$) the Gell-Mann & Brueckner (1957) formula

$$\epsilon_c = 0{\cdot}0622 \ln r_s - 0{\cdot}096 \tag{2·8}$$

was used. For the metallic density region ($2 \leqslant r_s \leqslant 5{\cdot}5$) the Bohm–Pines interpolation formula (Pines 1955; Nozières & Pines 1958) was considered the most suitable,

$$\epsilon_c = 0{\cdot}031 \ln r_s - 0{\cdot}115. \tag{2·9}$$

PHILOSOPHICAL TRANSACTIONS OF THE ROYAL SOCIETY A MATHEMATICAL, PHYSICAL & ENGINEERING SCIENCES

For the intermediate region $(1 \leqslant r_s \leqslant 2)$ a graphically interpolated function joining smoothly (2·8) and (2·9) was chosen. With $\epsilon_c(r_s)$ and the spatial density of electrons being known as a function of the radius from the nucleus, a perturbation potential (separation energy) was determined by

$$U = \epsilon_c(r_s) - \frac{1}{3}\frac{\mathrm{d}\epsilon_c}{\mathrm{d}\ln r_s} \tag{2·10}$$

from which the contribution of the uniformly distributed conduction electrons ($r_s = 2{\cdot}638$) was subtracted; they were already taken into account as item (i) of the potential. The perturbation calculation performed with this potential gave a maximum energy shift of 6×10^{-4} Ry, which is negligible compared with the other errors.

To compute the potential due to the Coulomb interaction of the conduction electrons (Hartree approximation), we first assume a spherically symmetric distribution of conduction electron around each nucleus (item (f)) and later compute the correction due to the lattice effects (item (g)). The potential to be considered was that seen by a small test charge and due to the averaged distribution of the conduction electrons assuming that they do not undergo exchange. This is a self-consistent problem and because of the laborious calculations involved it has never been rigorously solved for any metal. However, for aluminium Heine has achieved a rudimentary self-consistency within the desired accuracy (0·03 Ry) and from his calculation it is possible to see that a uniform distribution of electrons inside the Wigner–Seitz sphere is a very good approximation. The resulting error is less than 0·01 Ry. The uniform distribution assumption is known to be good for metals with no d-electrons (Callaway 1958). Moreover, magnesium is very similar to aluminium in many respects, and we can be confident that the assumption of a uniform distribution will give the same accuracy obtained for aluminium by Heine.

The solution of Poisson's equation

$$\nabla^2 U(\mathbf{r}) = -8\pi q \tag{2·11}$$

for a uniform charge density q corresponding to a total charge of two electrons inside the Wigner–Seitz sphere of radius $r_0 = 3{\cdot}324$ is

$$\left.\begin{aligned} 2Z_4(r) = -rU(r) &= \frac{2r}{r_0^3}(r^2 - 3r_0^2) \quad (r \leqslant r_0), \\ &= -4 \quad (r \geqslant r_0). \end{aligned}\right\} \tag{2·12}$$

Values of $2Z_4$ are given in table 4.

A potential due to a uniform density inside the Wigner–Seitz sphere is not entirely valid unless a correction is made for the region midway between the atoms. If we place a sphere of radius r_0 centred at each ion site, there will be regions in the metal where two neighbouring spheres overlap and other regions not covered by any sphere. We introduce an additional potential $2Z_5$ in order to correct for this effect. We followed a procedure similar to that used by Heine for aluminium, consisting of:

(a) Selection of a set of few points covering the whole lattice, mainly the region midway between nuclei.

(b) Calculation at these points of a potential $V_1(r)$ due to one proton at each lattice point and a uniform distribution of electrons corresponding to one electron per proton.

To compute V_1 we applied the Ewald technique as described by Kittel (1956), but replacing the lattice of negative ions by a uniform distribution of negative charge.

(*c*) Subtraction from V_1 of the potential V_2 due to one proton in each lattice point surrounded by a sphere of radius r_0 of uniform charge equivalent to one electron, thus a potential $V_3 = V_1 - V_2$ was obtained.

(*d*) Multiplication of V_3 by a suitable constant to take account of the real density of electrons in magnesium in the regions of the lattice where the correction is important.

(*e*) Selection of a constant C and values of a function $U_5(r)$ at certain values of r such that

$$V_3(\mathbf{r}) = C + \sum_{r_i} U_5(|\mathbf{r} - \mathbf{r}_i|) \tag{2·13}$$

agreed with the values of V_3 computed for the set of selected points. $U_5(r)$ was chosen to vanish for r greater than the maximum distance from any point in the crystal to the nearest ion site.

(*f*) Graphical interpolation of U_5 between the computed values and calculation of

$$2Z_5(r) = -rU_5(r).$$

Some values of $2Z_5$ are shown in table 4. This method gives a correction to $2Z_5$ such that the potential is computed exactly at the selected set of points and varies smoothly over the whole lattice. In this way we have corrected for lattice effects on the conduction electron distribution and still have kept the potential in the form (2·1) and (2·2).

The main source of errors in the potential turns out to be the contribution of exchange and correlation among conduction electrons. In fact the word 'potential' is misleading in this context, since correlation and exchange are many-body effects and must be treated as such. However, the contributions to the many-body treatment of electrons in metals (Falicov & Heine 1961) have shown that the independent particle approximation is still valid for 'dressed' electrons or holes near the Fermi surface. These 'dressed' particles or quasi-particles interact via a screened weak potential that can be considered as a perturbation on the independent particle model and treated in a low-order approximation, say the Hartree–Fock approximation. This screened electron-electron interaction gives rise to a modification of the single-particle band energies and as such must be considered in any band-structure calculation. However, the computation of this contribution for electrons in a lattice amounts to solving extremely difficult equations (Hubbard 1958) whose proper solution has not yet been attempted. Even for the case of free electrons, i.e. electrons moving in a background of uniformly distributed positive charge, the calculation of the single-particle energies is very difficult and the existing formulae are far from being accurate in comparison with the other terms in the band energies. From the various treatments of the electron-electron interaction we have chosen for the present calculation the formulae given by Bohm and Pines (Pines 1955) obtained through a collective motion approach. In choosing this approximation for magnesium metal we have introduced two different and appreciable errors: we have taken the errors inherent in the Bohm–Pines treatment and we have applied a free-electron formula to electrons that move in a crystal lattice. Bohm and Pines have estimated the error in the correlation energy to be about 15 %; the mean correlation energy in magnesium is about −0·085 Ry so that the error involved in the Bohm–Pines formula is about 0·013 Ry.

It is reasonable to apply the free-electron approximation to the conduction electrons in magnesium. The screening of the q Fourier components of the Coulomb interaction involves excitation of electrons by an amount q in k-space. Thus with q of the order k_F, this will involve a large fraction of the Fermi distribution. The resulting screened potential will therefore be very similar to that of a free-electron gas, differing say by a fraction of order ϵ, where ϵ is the fraction of the whole band structure which is severely disturbed by the presence of the energy gaps. In magnesium ϵ is small because of the small gaps. Thus the screening of the Coulomb potential is a property of the electron gas as a whole and not sensitive to the details of the band structure. We may therefore take what we suppose to be the free-electron screened potential.

We can now calculate the exchange between a Bloch state $\psi_{\mathbf{k}}$ and the whole Fermi distribution. Again there are the strong oscillations near the ion sites, in a volume about 10 % of the total volume of the crystal, which we neglect. The important result is: even when $\psi_{\mathbf{k}}$ has the form of a cosine- or sine-like function, i.e. a standing wave and not plane wave as in the free electron, because $\mathbf{k}$ is at or near the Brillouin zone boundary, the total exchange with the Fermi distribution is the same as for $\psi = \exp(i\mathbf{kr})$. Clearly there are interference effects when we calculate exchange between two standing waves $\cos \mathbf{k}_1\mathbf{r}$ and $\cos \mathbf{k}_2\mathbf{r}$, etc., but these all cancel out when the sum of $\mathbf{k}_2$ over the whole Fermi distribution is performed.

The formula for the one-electron correlation and exchange energy given by Bohm and Pines (Pines 1955) in the free-electron case is

$$V_{\text{B.P.}}(k) = -\frac{0{\cdot}611}{r_s}\left[2-4\beta+\frac{k_{\text{F.}}^2-k^2}{k_{\text{F.}}k}\ln\frac{k_{\text{F.}}+k}{k_{\text{F.}}-k}\right] \quad (0 \leqslant k \leqslant (1-\beta)\,k)$$

$$= -\frac{0{\cdot}611}{r_s}\left[1-2\beta+\frac{(\beta^2-1)\,k_{\text{F.}}^2+3k^2}{2kk_{\text{F.}}}+\frac{k_{\text{F.}}^2-k^2}{k_{\text{F.}}k}\ln\frac{k_{\text{F.}}+k}{\beta k_{\text{F.}}}\right] \quad ((1-\beta)\,k_{\text{F.}} \leqslant k \leqslant k_{\text{F.}}) \tag{2·14}$$

where $k_{\text{F.}}$ is the Fermi momentum, and

$$\beta = \alpha r_s^{\frac{1}{2}}. \tag{2·15}$$

Several values have been suggested for the constant α (Fletcher & Larson 1958). We have chosen the original value proposed by Bohm and Pines (Pines 1955),

$$\alpha = 0{\cdot}353.$$

TABLE 5. THE BOHM–PINES POTENTIAL

k	$V_{\text{B.P.}}(k)$	k	$V_{\text{B.P.}}(k)$
0·0	−0·3952	0·5	−0·2836
0·1	−0·3894	0·6	−0·2622
0·2	−0·3715	0·7	−0·2414
0·3	−0·3408	0·72	−0·2372
0·4	−0·3078		

With the approximation described above, the exchange and correlation among conduction electron can thus be described in terms of a potential that depends only on $\mathbf{k}$-vector. As such it does not contribute to the potential $2Z(r)$ shown in table 4 and it must be added to the final values of the energy computed by solving the secular equation as described in §3. Some values of $V_{\text{B.P.}}(k)$ as given by (2·14) are shown in table 5. The error in $V_{\text{B.P.}}$ which

PHILOSOPHICAL TRANSACTIONS OF THE ROYAL SOCIETY A MATHEMATICAL, PHYSICAL & ENGINEERING SCIENCES

is estimated to be of about 0·02 Ry, affects the overall band width but its effects on the shape of the Fermi surface are much less important.

Spin-orbit coupling needs special attention. The magnitude of the spin-orbit energy increases with atomic number. For silicon, with atomic number 14 which is the element of group IV closest to magnesium, the spin-orbit splitting at the top of the valence band amounts to 0·0026 Ry (Herman 1955): this is an order of magnitude smaller than our total error and would seem therefore to be negligible. However, it is well known that the presence of a spin-dependent term in the Hamiltonian may cause the splitting of some degeneracies in the band energy levels (Elliott 1954). This is particularly important in the h.c.p. structure, where the sticking-together of the bands at the hexagonal faces of the Brillouin zone is removed by spin-orbit effects (Cohen & Falicov 1960). We shall neglect the spin-orbit terms for the time being since its quantitative effects are small, but they will be reconsidered in § 6 when we analyze the topological properties of the Fermi surface.

3. The orthogonalized plane waves and the secular equation

Having computed the lattice potential $V(\mathbf{r})$, we compute in four steps the solution of the Schrödinger equation

$$[-\nabla^2+V(\mathbf{r})]\,\psi_{\mathbf{k}n}=E_{\mathbf{k}n}\psi_{\mathbf{k}n} \tag{3·1}$$

for the $24N$ electrons of the system, $2N$ being the number of atoms in the crystal:

(i) Determination of the Bloch tight-binding orbitals required to set up the *OPW*s,

(ii) selection and calculation of the *OPW*s (the basis functions),

(iii) setting up of the secular equation, which involves the calculation of the matrix elements of the Hamiltonian and the overlap matrix in terms of the *OPW*s,

(iv) solution of the secular equation.

All the numerical computations have been carried out in EDSAC 2; those concerned with item (i) were performed in a separate program. The remaining three items were computed in a single complete program, some of whose details are given in the present section.

Since the total potential $V(\mathbf{r})$ is expressed in the form (2·1) as a sum of atomic-like potentials, we first consider the solutions of the atomic-like Schrödinger equation

$$[-\nabla^2+U(r)]\,u_t=(-E_t)\,u_t \tag{3·2}$$

with E_t essentially positive. These solutions can be labelled according to the usual notation for atomic orbitals

$$t=1s,\quad 2s,\quad 2p_x,\quad 2p_y,\quad 2p_z;$$

they are the auxiliary 'core' functions which we shall need in setting up the *OPW*s (Heine 1957). We first build up Bloch orbitals out of the u_t, which are exact eigenfunctions of the crystal Hamiltonian (3·1) only if

$$\int u_t^*(\mathbf{r}-\mathbf{R}_\alpha)\,u_t(\mathbf{r}-\mathbf{R}_\beta)\,\mathrm{d}^3r=\delta_{\alpha\beta}, \tag{3·3}$$

$$\int |u_t(\mathbf{r}-\mathbf{R}_\alpha)|^2\,U(\mathbf{r}-\mathbf{R}_\beta)\,\mathrm{d}^3r=U_t\delta_{\alpha\beta}, \tag{3·4}$$

$$\int u_t^*(\mathbf{r}-\mathbf{r}_\alpha)\,U(\mathbf{r}-\mathbf{R}_\beta)\,u_t(\mathbf{r}-\mathbf{r}_\beta)\,\mathrm{d}^3r=U_t\delta_{\alpha\beta}, \tag{3·5}$$

i.e. there is no overlap between atomic functions or between atomic functions and potentials of different centres. Although it is not exactly so we assume in what follows that (3·3), (3·4) and (3·5) are valid for the first five eigenfunctions of (3·2). The error involved in this approximation is discussed in § 5.

Since the h.c.p. structure is not a simple Bravais lattice and has two atoms per unit cell, the atomic sites $\mathbf{R}_\alpha$ can be classified in two different groups. With the origin of the lattice vector system taken at one of the nuclei, the first group of atoms is formed by the atom at the origin and all the others whose positions are given by vectors of the hexagonal lattice:

$$\text{1st group:} \quad \mathbf{R}_\alpha = \mathbf{R}_i = l_i\mathbf{t}_1 + m_i\mathbf{t}_2 + n_i\mathbf{t}_3 \quad (l, m, n = \text{integers}).$$

Each atom of the second group is in a location that differs from a location of the first set by a vector

$$\left.\begin{aligned} \boldsymbol{\tau} &= \tfrac{1}{2}\mathbf{t}_1 + \tfrac{1}{3}\mathbf{t}_2 + \tfrac{2}{3}\mathbf{t}_3; \\ \text{2nd group;} \quad \mathbf{R}_\alpha &= \mathbf{R}_i + \boldsymbol{\tau}. \end{aligned}\right\} \tag{3·6}$$

Hence two different sets of Bloch orbitals exist for each solution of (3·2). These are

$$\left.\begin{aligned} (\Phi_{1t}, \mathbf{k}) &= N^{-\frac{1}{2}} \sum_i u_t(\mathbf{r} - \mathbf{R}_i) \exp(\mathrm{i}\mathbf{k}\mathbf{R}_i), \\ (\Phi_{2t}, \mathbf{k}) &= N^{-\frac{1}{2}} \sum_i u_t(\mathbf{r} - \mathbf{R}_i - \boldsymbol{\tau}) \exp(\mathrm{i}\mathbf{k}\mathbf{R}_i). \end{aligned}\right\} \tag{3·7}$$

With the assumptions (3·3) to (3·5), these functions are normalized and orthogonal to each other:

$$\int (\Phi_{st}, \mathbf{k})^* (\Phi_{s't'}, \mathbf{k}') \, \mathrm{d}^3 r = \delta_{\mathbf{k}\mathbf{k}'} \delta_{ss'} \delta_{tt'},$$

and are solutions of (3·1) with

$$E_{1kt} = E_{2kt} = (-E_t). \tag{3·8}$$

To solve (3·2) we have applied the standard techniques used for the calculation of atomic structures (Hartree 1957). The functions u_t are expressed in the form

$$u_t(\mathbf{r}) = (1/r) P_t(r) Y_t(\theta, \phi), \tag{3·9}$$

where the Y's are normalized spherical harmonics. The results for $P_t(r)$ and the corresponding energies E_t are shown in table 6. It is worth noting that while assumptions (3·3), to (3·5) are very well satisfied for the 1s-function because of the negligible values of P_{1s} in the region $r \simeq 3$, this is not so for the 2s- and 2p-functions and the consequent contribution to the total error must be taken into account.

We define the orthogonalized plane wave of vector $\mathbf{k}$ by

$$(OPW, \mathbf{k}) = A_{\mathbf{k}} [\Omega^{-1} \exp(\mathrm{i}\mathbf{k}\mathbf{r}) - \sum_{ts} B_{st\mathbf{k}} (\Phi_{st}, \mathbf{k})], \tag{3·10}$$

where Ω is the volume of the crystal,

$$t = 1s, \quad 2s, \quad 2p_x, \quad 2p_y, \quad 2p_z,$$
$$s = 1, \quad 2,$$

and the $(\Phi_{st}, \mathbf{k})$ are defined by (3·7). This is not the only definition that has been used. The Bloch functions to which the OPWs are orthogonalized do not necessarily have to be the 'core' solutions of (3·1). There is a complete freedom to choose them (Woodruff 1957).

But, as proved by Heine (1957), (3·10) is the simplest and most natural formulation and the one that gives the best convergence for the resulting secular equation.

The orthogonality and normalization condition that determine $A_{\mathbf{k}}$ and $B_{st\mathbf{k}}$ are

$$\int (OPW, \mathbf{k})^* \, (\Phi_{st}, \mathbf{k}) \, \mathrm{d}^3 r = 0, \tag{3·11}$$

$$\int |(OPW, \mathbf{k})|^2 \, \mathrm{d}^3 r = 1. \tag{3·12}$$

TABLE 6. THE ATOMIC-LIKE FUNCTIONS FOR THE CORE ELECTRONS

	P_{1s}	P_{2s}	P_{2p}
energy	91·022	5·639	3·177
r			
0	0·00	0·00	0·00
0·01	$7{\cdot}75 \times 10^{-1}$	$1{\cdot}94 \times 10^{-1}$	$5{\cdot}47 \times 10^{-3}$
0·03	1·83	$4{\cdot}54 \times 10^{-1}$	$4{\cdot}37 \times 10^{-2}$
0·06	2·57	$6{\cdot}03 \times 10^{-1}$	$1{\cdot}47 \times 10^{-1}$
0·10	2·68	$5{\cdot}30 \times 10^{-1}$	$3{\cdot}29 \times 10^{-1}$
0·15	2·27	$2{\cdot}31 \times 10^{-1}$	$5{\cdot}68 \times 10^{-1}$
0·30	$8{\cdot}40 \times 10^{-1}$	$-7{\cdot}84 \times 10^{-1}$	1·09
0·50	$1{\cdot}58 \times 10^{-1}$	−1·34	1·28
0·80	$1{\cdot}07 \times 10^{-2}$	−1·09	1·00
1·20	$2{\cdot}47 \times 10^{-4}$	$-4{\cdot}89 \times 10^{-1}$	$4{\cdot}98 \times 10^{-1}$
1·60	$5{\cdot}63 \times 10^{-6}$	$-2{\cdot}08 \times 10^{-1}$	$2{\cdot}51 \times 10^{-1}$
2·00	$1{\cdot}31 \times 10^{-7}$	$-8{\cdot}49 \times 10^{-2}$	$1{\cdot}24 \times 10^{-1}$
3·00	$1{\cdot}73 \times 10^{-11}$	$-8{\cdot}36 \times 10^{-3}$	$2{\cdot}07 \times 10^{-2}$
4·00	$2{\cdot}32 \times 10^{-15}$	$-7{\cdot}87 \times 10^{-4}$	$3{\cdot}39 \times 10^{-2}$
5·00	$6{\cdot}91 \times 10^{-19}$	$-7{\cdot}42 \times 10^{-5}$	$5{\cdot}58 \times 10^{-4}$

With the definition

$$b_{t\mathbf{k}} = \Omega_0^{-\frac{1}{2}} \int u_t^*(\mathbf{r}) \exp(\mathrm{i}\mathbf{k}\mathbf{r}) \, \mathrm{d}^3 r, \tag{3·13}$$

(3·11) and (3·12) reduce to

$$B_{1t\mathbf{k}} = 2^{-\frac{1}{2}} b_{t\mathbf{k}}, \tag{3·14}$$

$$B_{2t\mathbf{k}} = 2^{-\frac{1}{2}} b_{t\mathbf{k}} \exp(\mathrm{i}\mathbf{k}\boldsymbol{\tau}), \tag{3·15}$$

where $\boldsymbol{\tau}$ is defined by (3·16), and

$$A_{\mathbf{k}} = [1 - \sum_t (b_{t\mathbf{k}})^2]^{-\frac{1}{2}}. \tag{3·16}$$

To compute (3·13) it is convenient to express u_t in the form (3·9) and to expand the exponential function in the well-known series of spherical waves. With the use of the orthogonality properties of the spherical harmonics the final integrals to be evaluated are:

(*a*) for $\mathbf{k} \neq 0$

$$b_{1s,\mathbf{k}} = \left(\frac{3}{r_0^3}\right)^{\frac{1}{2}} \frac{1}{|k|} \int_0^\infty P_{1s}(r) \sin(|k| r) \, \mathrm{d}r; \tag{3·17}$$

similarly for $2s$,

$$b_{2px,\mathbf{k}} = \frac{3}{(r_0)^{\frac{3}{2}}} \frac{k_x}{|k|^2} \int_0^\infty P_{2p}(r) \left[\frac{\sin(|k| r)}{|k| r} - \cos(|k| r)\right] \mathrm{d}r, \tag{3·18}$$

and similarly for $2p_y$ and $2p_z$.

(*b*) For $\mathbf{k} = 0$

$$b_{1s,0} = \left(\frac{3}{r_0^3}\right)^{\frac{1}{2}} \int_0^\infty P_{1s}(r)\,\mathrm{d}r \tag{3·19}$$

and similarly for 2*s*,

$$b_{2px,0} = b_{2py,0} = b_{2pz,0} = 0. \tag{3·20}$$

In the above formulae r_0 is the Wigner–Seitz radius.

If we consider the *OPW*s as a complete system of basis functions for the conduction electron the band energy eigenvalues are given by the roots of the secular equation

$$|H_{mn} - ES_{mn}| = 0, \tag{3·21}$$

where H_{mn} is a matrix element of the Hamiltonian between two *OPW*s, and S_{mn} is the element of the overlap matrix between the same two functions. Owing to the translational symmetry of the lattice, the only non-zero matrix elements are those connecting *OPW*s in which the **k**-vectors differ by a reciprocal lattice vector $\mathbf{G}_i$. The secular equation is then factorized and for each $\mathbf{k}_m$ of the extended zone scheme only vectors of the form

$$\mathbf{k}_n = \mathbf{k}_m + \mathbf{G}_i$$

are to be considered. With the notation

$$\mathbf{G}_{mn} \equiv \mathbf{k}_n - \mathbf{k}_m, \tag{3·22}$$

the matrix elements

$$S_{mn} = \int (OPW, \mathbf{k}_m)^* \, (OPW, \mathbf{k}_n)\,\mathrm{d}^3r, \tag{3·23}$$

$$H_{mn} = \int (OPW, \mathbf{k}_m)^* \, H(OPW, \mathbf{k}_n)\,\mathrm{d}^3r, \tag{3·24}$$

turn out to be

$$S_{mn} = -\tfrac{1}{2} A_{\mathbf{k}_m} A_{\mathbf{k}_n} \mathscr{S}(\mathbf{G}_{mn}) \sum_t b_{t\mathbf{k}_m} b_{t\mathbf{k}_n} \quad \text{for} \quad m \neq n, \tag{3·25}$$

$$S_{mm} = 1, \tag{3·26}$$

$$H_{mn} = \tfrac{1}{2} A_{\mathbf{k}_m} A_{\mathbf{k}_n} \mathscr{S}(\mathbf{G}_{mn}) \left[(\mathbf{k}_m)^2 \delta_{mn} + \sum_t b_{t\mathbf{k}_m} b_{t\mathbf{k}_n} E_t + (U, \mathbf{G}_{mn})\right], \tag{3·27}$$

where $\mathscr{S}(\mathbf{G}) = 1 + \exp\left[-2\pi\mathrm{i}(\tfrac{1}{2}h + \tfrac{1}{3}k + \tfrac{2}{3}l)\right]$ (with $\mathbf{G} = h\mathbf{G}_1 + k\mathbf{G}_2 + l\mathbf{G}_3$) (3·28)

is the usual structure factors of the reciprocal lattice vector **G**. Also

$$\left.\begin{aligned} (U, \mathbf{G}) &= -\frac{3}{r_0^3 |\mathbf{G}|} \int_0^\infty 2Z_p(r) \sin(|\mathbf{G}| r)\,\mathrm{d}r \quad (|\mathbf{G}| \neq 0) \\ \text{and} \qquad (U, 0) &= -\frac{3}{r_0^3} \int_0^\infty 2Z(r)\, r\,\mathrm{d}r \end{aligned}\right\} \tag{3·29}$$

are the Fourier coefficients of the potential. The integrals (3·29) have been evaluated for 43 essentially different values of $|\mathbf{G}|$, equivalent to 465 vectors of the reciprocal lattice. Some values are shown in table 7.

Owing to the limitations of the computer it was decided to use for general points of the Brillouin zone a secular equation of twelfth order. Consequently twelve reciprocal lattice vectors had to be chosen for each point, so as to obtain in each case the twelve total vectors $\mathbf{k} + \mathbf{G}$ of smallest length. However, since only one general program for all the points was

used, the selection of the lattice vectors was made so as to fit the requirements of most of the zone. Owing to the symmetry, values of the energy have to be computed only in one-twenty-fourth of the reduced zone. This region was chosen to be the triangular prism determined by the six points $\Gamma AMLKH$ of table 3, and the 12 reciprocal vectors were selected to fit, as an average, the requirement of shortest length for most of the points of this prism.

TABLE 7. FOURIER COEFFICIENTS OF THE POTENTIAL

h	k	l	$\lvert\mathbf{G}\rvert$	$(U, \mathbf{G})$	$\mathscr{S}(\mathbf{G})$
0	0	0	0·000	0·7068	2
1	0	0	0·642	0·5742	0
0	1	0	1·204	0·3719	$0{\cdot}5 \pm i\alpha$
2	0	0	1·284	0·3475	2
1	1	0	1·365	0·3252	$1{\cdot}5 \pm i\alpha$
2	1	0	1·761	0·2444	$0{\cdot}5 \pm i\alpha$
3	0	0	1·927	0·2229	0
0	1	1	2·085	0·2069	2
1	1	1	2·182	0·1987	0

$\alpha = \frac{1}{2}\sqrt{3}$.

To determine the energy and wave function at a given $\mathbf{k}$ it is necessary to solve the secular equation

$$(H - ES)\, u = 0 \tag{3·30}$$

finding both eigenvalues E_m and eigenvectors u_m. The solution of this problem is not straightforward. Standard numerical techniques for the solution of secular equations were available only for the case of Hermitian matrices $H^+ = H$ and unit overlap matrix $S_{mn} = \delta_{mn}$. In our case the second condition was not fulfilled and the available routine could not be used. If the matrices are multiplied by S^{-1} it is possible to transform S into the unit matrix, but the resulting Hamiltonian HS^{-1} is no longer Hermitian. The only possible way of solving the complete problem is then to find a unitary matrix T such that $TST^{-1} = I$ and solve the secular equation

$$(THT^{-1} - EI)\, u' = 0.$$

Finding T is equivalent to a Schmidt orthogonalization process, i.e. finding of a set of linear combination of OPWs such that any two linear combinations are orthogonal. This is a very cumbersome task which involves an unnecessary amount of trouble and requires much running time in the computer.

However, if only eigenvalues are required, i.e. if we need only values of the energy and not the wave functions, the matrix calculation can be reduced to an algebraic one. The energies are given by the roots of the equation

$$\det |H - ES| = 0. \tag{3·31}$$

This is the most convenient method for our purposes. The evaluation of 12×12 complex determinants only takes times of the order of one second in EDSAC 2.

The calculation of $E(\mathbf{k})$ has been performed in the computer for 53 different points of the chosen region of the Brillouin zone. The energies at the six symmetry points have been computed separately, and full account of them is given in the next section. The calculation was performed by means of a single program of about 1950 words which, for a given

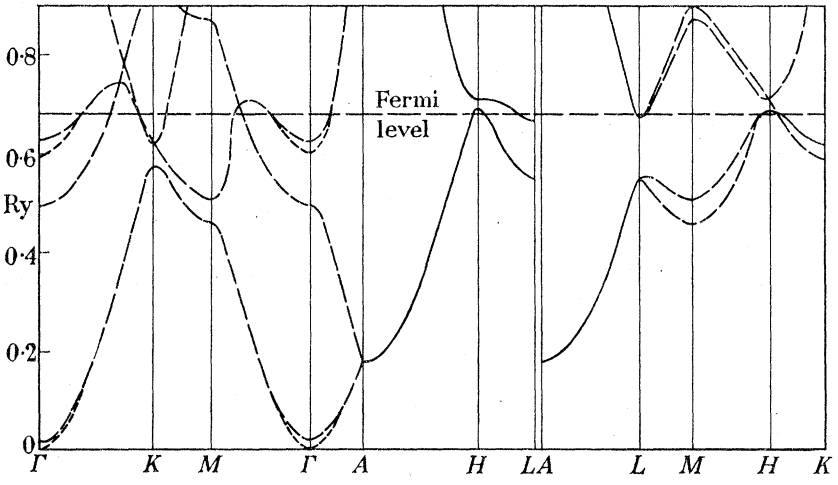

FIGURE 2. The band energy values E in magnesium with correlation and exchange along various lines of the Brillouin zone. The broken lines represent single levels and the full lines double-degenerate states. Near Γ in the first and third zone the two curves represent E as computed with the general program (upper curve) and the more accurate group theoretical method (lower curve).

TABLE 8. BAND ENERGY AT POINTS OF SYMMETRY

point	E'	E	n	D	S
Γ	0·000	0·000	1	1	Γ_1^+
	0·352	0·494	2	1	Γ_3^+
	0·455	0·597	3	1	Γ_4^-
A	0·116	0·178	1, 2	2	A_1
M	0·325	0·458	1	1	M_1^+
	0·369	0·502	2	1	M_2^-
	0·684	0·875	3	1	M_4^-
	0·709	0·900	4	1	M_3^+
	0·767	0·958	5	1	M_2^-
L	0·397	0·547	1, 2	2	L_1
	0·517	0·667	3, 4	2	L_1
K	0·425	0·578	1	1	K_1
	0·466	0·618	2, 3	2	K_5
H	0·519	0·686	1, 2	2	H_2
	0·541	0·708	3, 4	2	H_1
	0·731	0·898	5, 6	2	H_3

E' Energy values (rydbergs) without correlation and exchange, referred to the bottom of the band.
E Energy values (rydbergs) with correlation and exchange, referred to the bottom of the band.
n Band index.
D Degeneracy of the level.
S Symmetry of the level.

k-vector, evaluated the energy levels in the range 0 to 1 Ry counting from the bottom of the band. This program consisted essentially of

(*a*) Numerical information: values of the functions P_{1s}, P_{2s} and P_{2p} and their corresponding energies, structure factors and Fourier coefficients of the potential, intervals of integration and lattice constants.

(*b*) Subroutine to control the transfer to and from the auxiliary store.

(*c*) Subroutine to calculate the coefficients of the *OPW*s by means of equations (3·13) to (3·20).

(d) Subroutine to build up the matrix elements of the Hamiltonian and the overlap matrix by means of (3·25), (3·26) and (3·27).

(*e*) Subroutine to evaluate the determinant (3·31) with tentative values of the energy.

(*f*) Subroutine to find the roots of the determinantal equation with an accuracy of 10^{-4} Ry and print them.

(*g*) Master routine to call the different subroutines in turn and repeat the whole process for each value of **k**.

The final values of the energy, including correlation and exchange and referred to the bottom of the band are given in figure 2. The values of the energy at the symmetry points as described in the next section are given in table 8.

4. Group-theory considerations

The h.c.p. lattice remains invariant under a certain number of spatial transformations. These operations form a space group G, known in the international notation as $P6_3/mmc$ and in the Schoenflies notation as D^4_{6h}.

The main proposition of group theory that we apply to our case establishes that the eigenvectors of any operator invariant under given group of transformations, may be chosen to transform under the operations of the group according to one of its irreducible representations.

Consider first the elements of G consisting only of pure translations. These elements form a subgroup T of G that is invariant and Abelian; its irreducible representations are all one-dimensional and the corresponding eigenvectors are Bloch functions with **k**-vectors defined in the first Brillouin zone. Since the Hamiltonian is invariant under the operations of T, the wave functions of the electrons in the lattice are Bloch orbitals. The corresponding energy eigenvalues can thus be labelled by their **k**-vectors. This is, of course, the Bloch theorem, basis of the electron theory of solids.

Since we are interested in the values $E(\mathbf{k})$, in what follows we do not mix wave functions of different **k**-vectors in the reduced zone scheme. From all the transformations of G we are only concerned with those that leave **k** invariant. For a given **k**, these operations form a group $G^{\mathbf{k}}$ which, according to Bouckaert, Smoluchowski & Wigner (1936), describes all the symmetry properties of the wave functions. It is evident that $G^{\mathbf{k}}$ contains T as an invariant subgroup. From all the translations of T, those satisfying the relation

$$\mathbf{t}.\mathbf{k} = 2\pi n \quad (n = \text{integer}) \tag{4·1}$$

form an invariant subgroup $T^{\mathbf{k}}$. If we use Bloch functions of vector **k**, the representation of all the elements of $T^{\mathbf{k}}$ is unity. Thus, we consider all the translations of $T^{\mathbf{k}}$ as the identity, so that the factor group $G^{\mathbf{k}}/T^{\mathbf{k}}$ is now a group and the only one that remains to be considered.

If a given representation D of $G^{\mathbf{k}}/T^{\mathbf{k}}$ is n-dimensional, there are n different wave functions which transform according to D and have the same energy eigenvalue. This means that the existence of an n-dimensional representation yields an n-degenerate energy level. On the other hand, a function transforming according to a one-dimensional representation gives

in general a non-degenerate level, except where other symmetry operations of the Hamiltonian exist or when accidental degeneracy occurs.

Tables of characters of the $G^{\mathbf{k}}/T^{\mathbf{k}}$ groups in the h.c.p. lattice were given by Herring (1942), who also studied compatibility relations between different points of the Brillouin zone. For the sake of simplicity consider the case $\mathbf{k} = 0$. Here $T^0 = T$ and the group G^0/T^0 is simply the point group of the lattice: 6/mmm or D_{6h}.† If we try to determine the wave functions at $\mathbf{k} = 0$ by expansion in series of *OPW*s, this would in general look like

$$\begin{aligned}\psi^n_{\mathbf{k}=0} &= A^n_0(OPW, \mathbf{O}) + A^n_{\mathbf{G}_1}(OPW, \mathbf{G}_1) + A^n_{-\mathbf{G}_1}(OPW, -\mathbf{G}_1) + \ldots \\ &= \sum_i A^n_{\mathbf{G}_i}(OPW, \mathbf{G}_i),\end{aligned} \tag{4·2}$$

where n determines the band and $\mathbf{G}_i$ are reciprocal lattice vectors. Through group theoretical analysis we know that each *OPW* transforms according to some irreducible representations of G^0/T^0. For example:

$(OPW, 0)$ transforms according to Γ_1^+,

$(OPW, \mathbf{G}_1)$ and $(OPW, -\mathbf{G}_1)$ transform according to $\Gamma_3^+ + \Gamma_4^-$,

$(OPW, 2\mathbf{G}_1)$ and $(OPW, -2\mathbf{G}_1)$ transform according to $\Gamma_1^+ + \Gamma_2^-$.

Thus for the bottom of the band, which has Γ_1^+ symmetry, the coefficients of $(OPW, \mathbf{G}_1)$ and $(OPW, -\mathbf{G}_1)$ must be zero since for any given symmetry no contributions from other symmetries appear. On the other hand, $(OPW, 2\mathbf{G}_1)$ and $(OPW, -2\mathbf{G}_1)$ will give a contribution, but only through the linear combination that has Γ_1^+ symmetry, i.e.

$$[(OPW, 2\mathbf{G}_1) + (OPW, -2\mathbf{G}_1)].$$

In general, from all the M $\mathbf{k}$-vectors differing by a reciprocal lattice vector and having the same modulus we can form N_s linear combinations ($N_s \leqslant M$; in most cases $N_s = 1$) which have a given symmetry S, i.e. transform according to the S irreducible representation of $G^{\mathbf{k}}/T^{\mathbf{k}}$. The series for the wave function for $\mathbf{k} = 0$ now looks like

$$\psi^{Sn}_{\mathbf{k}=0} = \sum_{|\mathbf{G}_i|} \sum_{l=1}^{N_S} B^{Sn}_{l|\mathbf{G}_i|}(LCOPW; S, l; |\mathbf{G}_i|), \tag{4·3}$$

where $(LCOPW; S, l; |\mathbf{G}_i|)$ denotes one of the N_S linear combinations of *OPW*s transforming according to the S irreducible representation. By means of this analysis the number of coefficients to be determined is greatly reduced and consequently the convergence of the series greatly improved; i.e. by solving a 12×12 secular equation based on 12 *LCOPW*s, one is effectively including a much larger number of *OPW*s and hence getting a better convergence.

This method, however, is only effective for points of high symmetry in the Brillouin zone, where $G^{\mathbf{k}}/T^{\mathbf{k}}$ contains several symmetry operations. For a general point of the zone $G^{\mathbf{k}}/T^{\mathbf{k}}$ is only the identity operator; only one irreducible representation exists and no reduction of the series is obtained for them. At points of high symmetry the group theoretical analysis allows a much better accuracy in the determination of the energy levels. As an example, the secular equations computed for the first three levels at $\mathbf{k} = 0$ were respectively of sixth, fourth, and fifth order, yet they are equivalent to a 43×43 secular equation for a

† We must note that this is not exactly true because some of the operations of G^0/T^0 have, in addition to the rotation, reflexion or inversion corresponding to 6/mmm, an additional translation $\boldsymbol{\tau}$.

PHILOSOPHICAL TRANSACTIONS OF THE ROYAL SOCIETY A MATHEMATICAL, PHYSICAL & ENGINEERING SCIENCES

general point. As mentioned in the preceding section, the secular equation computed for a general point was of twelfth order. The error due to the trunaction of the series can be evaluated by comparison with the high symmetry points, as shown in the next section.

The symmetry analysis of the wave functions at the six symmetry points of the h.c.p. Brillouin zone has been carried out using the character tables† given by Herring (1942). The values of the computed energies appear in table 8.

Some other properties of the energy values can be obtained from group theoretical considerations. When we move in **k**-space from a symmetry point P along one line of symmetry L, each representation of G^P/T^P splits in only one way into one or several representations of G^L/T^L. Each of these representations varies continuously along L. If L ends in another symmetry point P', one or several representations of G^L/T^L coallesce into one given representation of $G^{P'}/T^{P'}$. Thus, if a given symmetry P_A of P can be transformed into a symmetry P'_B of P' continuously along L we say that P_A and P'_B are compatible along L. Compatibility relations between symmetry points and the irreducible representations along the symmetry

TABLE 9. COMPATIBILITY RELATIONS BETWEEN POINTS OF SYMMETRY ALONG SYMMETRY LINES

to / from	Γ_1^+	Γ_3^+	Γ_4^-	A_1	M_1^+	M_2^-	M_3^+	M_4^-	L_1	K_1	K_5	H_1	H_2	H_3
Γ_1^+	—	—	—	Δ_1	Σ_1	Σ_1	—	—	—	T_1	T_1	—	—	—
Γ_3^+	—	—	—	Δ_2	—	—	Σ_3	Σ_3	—	—	—	—	—	—
Γ_4^-	—	—	—	Δ_2	Σ_1	Σ_1	—	—	—	—	T_4	—	—	—
A_1	$\Delta_{1,2}$	$\Delta_{1,2}$	$\Delta_{1,2}$	—	—	—	—	—	$R_{1,3}$	—	—	S_1	S_1	S_1
M_1^+	Σ_1	—	Σ_1	—	—	—	—	—	U_1	T_1	T_1	—	—	—
M_2^-	Σ_1	—	Σ_1	—	—	—	—	—	U_2	—	T_4	—	—	—
M_3^+	—	Σ_3	—	—	—	—	—	—	U_2	—	—	—	—	—
M_4^-	—	Σ_3	—	—	—	—	—	—	U_1	—	—	—	—	—
L_1	—	—	—	$R_{1,3}$	$U_{1,2}$	$U_{1,2}$	$U_{1,2}$	$U_{1,2}$	—	—	—	S_1	S_1	S_1
K_1	T_1	—	—	—	T_1	—	—	—	—	—	—	P_1	—	—
K_5	T_1	—	T_4	—	T_1	T_4	—	—	—	—	—	—	P_3	P_3
H_1	—	—	—	S_1	—	—	—	—	S_1	$P_{1,2}$	—	—	—	—
H_2	—	—	—	S_1	—	—	—	—	S_1	—	P_3	—	—	—
H_3	—	—	—	S_1	—	—	—	—	S_1	—	P_3	—	—	—

S_1 and P_3 are two-dimensional representations.
R_1 and R_3 appear together due to time reversal.

lines are given in table 9. The help of these relations in drawing the $E(\mathbf{k})$ curves comes from the two fundamental properties:

(*a*) Two energy levels at different symmetry points can be joined by continuous values of $E(\mathbf{k})$ along a symmetry line only if they are compatible.

(*b*) Two curves $E(\mathbf{k})$ with the same symmetry along a symmetry line never cross each other.

Further useful information obtained from group theoretical considerations is the degeneracy of the levels. Degenerate levels at a given **k** can be classified in three different types:

(*a*) degeneracy due to n-dimensional representations of $G^{\mathbf{k}}/T^{\mathbf{k}}$,

† Owing to the length of the tables of coefficients of the linear combinations of *OPW*s, they are omitted in the present paper. They can be obtained from the author by request.

(*b*) degeneracy due to time reversal symmetry,

(*c*) accidental degeneracy.

The first class only occurs at the symmetry points Γ, A, L, K, H, and along the lines HK, AH and HL, where multiple representations of $G^{\mathbf{k}}/T^{\mathbf{k}}$ exist; at A, L and H and along AH and HL all the representations are two- or four-dimensional.

Time reversal symmetry introduces additional degeneracies. By applying Herring's test (1937*a*) to study the doubling of levels (without spin) due to time reversal, it is readily shown that at a general point of the hexagonal face there is an additional pairing of levels. This is also true for the AL line where either R_1 and R_3 or R_2 and R_4 appear always together.

The fact that at the hexagonal face all the levels are degenerate implies that no energy gap exists there, and the energy as well as the wave functions change continuously going across the AHL plane. To represent energy surfaces it is thus convenient to take in **k**-space not simply a Brillouin zone but a region formed by two Brillouin zones contacting through their hexagonal faces. This representation has been used in the present work to describe the Fermi surface; it has been used before by Harrison (1960). However, it must be pointed out that when spin-orbit effects are taken into account, these considerations are no longer valid. Instead of considering the single groups given by Herring (1942), the analysis carried above must be done with the so-called double groups (Elliott 1954). It is thus proved that the bands no longer stick together at the hexagonal face, except along the lines AL. The presence of the spin-orbit term in the Hamiltonian is responsible for the existence of additional band gaps which, although very small (Cohen & Falicov 1960), introduce fundamental changes in the topology of the Fermi surface. However, for the purposes of comparison with already existing work we keep the double-zone representation pointing out in §6 the main consequences of spin-orbit coupling. Full account of these effects will be published elsewhere.

The third kind of degeneracy, i.e. accidental degeneracy, has also been described by Herring (1937*b*) and is due to the compatibility relations between levels at points of symmetry. For example, in the present calculation the four non-degenerate levels Γ_3^+, Γ_4^-; M_2^-, M_4^- are compatible along ΓM only in pairs $\Gamma_3^+ M_4^-$, $\Gamma_4^- M_2^-$ according to table 9. Thus along ΓM there are two continuous curves $E(\mathbf{k})$ joining the members of each pair: the symmetry of these lines are Σ_3 and Σ_1, respectively. Owing to the values of the energy at the ends of these lines, they must cross each other at some intermediate point, giving rise to a degenerate level.

Several accidental degeneracies appear in figure 2. They only occur at symmetry lines, symmetry planes or zone boundaries where at least two different irreducible representations of $G^{\mathbf{k}}/T^{\mathbf{k}}$ exist.

To end this section we may mention that the compatibility relations together with the periodicity of the system and the continuity of $E(\mathbf{k})$ gives useful information about the slopes of $E(\mathbf{k})$ curves at points of symmetry. For example:

(*a*) $E(\mathbf{k})$ has zero slope at M along the three symmetry lines ΓM, MK, ML, i.e. $E(\mathbf{k})$ has an extremum or a saddle point at M;

(*b*) along ΓK the slope of each curve $E(\mathbf{k})$ at K is equal to the slope of one of the curves $E(\mathbf{k})$ along KM which has the same value at K;

PHILOSOPHICAL TRANSACTIONS OF THE ROYAL SOCIETY A MATHEMATICAL, PHYSICAL & ENGINEERING SCIENCES

(*c*) Each pair of curves that comes to the same value of A along ΓA, have their slopes of equal modulus and opposite sign.

Several other similar relations are found; they have been employed in drawing the curves of figure 2.

5. Errors

The final errors in the values $E(\mathbf{k})$ come from the following sources:

(*a*) the errors in the potential,

(*b*) rounding off and truncation errors in the numerical procedures employed,

(*c*) the overlap of the atomic-like wave functions,

(*d*) the approximation of the infinite-order secular equation by one of finite order.

The errors in the evaluation of the lattice potential have been discussed in §2. From the eleven items enumerated, (*a*), (*b*), (*c*) and (*g*) give no appreciable error. Item (*d*) gives negligible error for the *s*-like states, and yields an error of less than 0·01 Ry for states of other symmetries. Items (*e*) and (*g*) can be neglected without appreciable error. The main error comes from the exchange and correlation terms (*h*) and (*i*) and has been estimated to be of the order of 0·02 Ry. For items (*f*) and (*k*) we may conclude from Heine's rudimentary self-consistency for aluminium that our error is not more than 0·01 Ry. Consequently, the total error due to the potential is about 0·03 Ry.

Rounding off and truncation errors were at all stages of the calculation negligibly small. The long storage locations of EDSAC 2 and the standard routines used for the calculation as well as the chosen intervals of integration ensure an accuracy of the numerical results such that no appreciable error was introduced.

Consider now the error introduced by the assumptions (3·3), (3·4) and (3·5). If we keep the definition of *OPW*s given in §3 and remove the above-mentioned conditions, the energy associated with a single *OPW* is now given by

$$\frac{\int (OPW, \mathbf{k}_m)^* \, H(OPW, \mathbf{k}_m) \, \mathrm{d}^3 r}{\int (OPW, \mathbf{k}_m)^* \, (OPW, \mathbf{k}_m) \, \mathrm{d}^3 r} \tag{5·1}$$

and the error to be considered is the difference between (5·1) and the matrix element H_{mm} as given by (3·27). The calculation of this error implies the evaluation of three different kinds of integrals:

$$\int u_t^*(\mathbf{r}-\mathbf{R}_\alpha) \, u_{t'}(\mathbf{r}) \, \mathrm{d}^3 r, \tag{5·2}$$

$$\int U(\mathbf{r}-\mathbf{R}_\alpha) \, u_t(\mathbf{r}) \exp(-\mathrm{i}\mathbf{k}\mathbf{r}) \, \mathrm{d}^3 r, \tag{5·3}$$

$$\int U(\mathbf{r}-\mathbf{R}_\alpha) \, u_t^*(\mathbf{r}-\mathbf{R}_\beta) \, u_t(\mathbf{r}) \, d^3 r, \tag{5·4}$$

where $\mathbf{R}_\alpha$ and $\mathbf{R}_\beta$ are vectors joining two different ion sites. The evaluation of these integrals is not straightforward and some approximations must be made. It is easily seen that the main contribution comes from (5·3) and $t = 2s, 2p$. An estimation of that integral shows that the total amount of correction is of the order of, but less than 0·003 Ry, which is negligible compared with the other errors.

The main error in the computation seems to be the convergence of the series, i.e. the error caused by approximating the infinite-order secular equation by the first twelve terms. To evaluate this error, values of the energy at symmetry points extrapolated from values along symmetry lines were compared with more accurate computations using the group theoretical analysis of § 4. The results obtained are shown in table 10. The errors are in general less than 0·015 Ry, except for two levels at Γ where the discrepancies appear puzzlingly large.

TABLE 10. RATE OF CONVERGENCE OF SECULAR EQUATIONS

level	value of best approximation evaluated	number of *OPW*s involved	value of 12×12 secular eqn.	error
Γ_1^+	0·000	43	0·022	−0·022
Γ_3^+	0·352	43	0·353	−0·001
Γ_4^-	0·455	43	0·489	−0·034
M_1^+	0·325	24	0·332	−0·007
M_2^-	0·369	24	0·381	−0·012
M_4^-	0·684	24	0·685	−0·001
M_3^+	0·709	24	0·710	−0·001
K_1	0·425	48	0·430	−0·005
K_5	0·466	48	0·478	−0·012
A_1	0·116	28	0·121	−0·005
L_1	0·397	16	0·406	−0·009
L_1	0·517	16	0·530	−0·013

TABLE 11. RATE OF CONVERGENCE OF SECULAR EQUATIONS

level	order secular equation	number of *OPW*'s	value of energy (arbitrary origin)	difference
Γ_1^+	1	1	−0·1485	—
s-like	2	9	−0·1508	0·0023
	3	11	−0·1545	0·0037
	4	23	−0·1718	0·0173
	5	35	−0·1764	0·0046
	6	43	−0·1824	0·0060
Γ_3^+	1	3	0·1698	—
p-like	2	23	0·1669	0·0029
	3	35	0·1659	0·0010
	4	43	0·1656	0·0003
Γ_4^-	1	3	0·3611	—
s-like	2	9	0·2976	0·0635
	3	23	0·2836	0·0140
	4	35	0·2731	0·0105
	5	43	0·2730	0·0001

A separate test was carried out for the three Γ levels to check the convergence of the secular equation. Values of the energy were evaluated with different approximations and the results are shown in table 11. We can see that while the convergence is very good for Γ_3^+ (*p*-like symmetry), for the two *s*-like levels the series converges slowly. No satisfactory explanation of this puzzle has been found. Ignoring these two anomalous values we can estimate the error due to convergence to be about 0·015 Ry. Then, in general, summing up all the contributions, the calculated values of the band energies as expressed in figure 2 have an accuracy of about 0·035 Ry.

6. Fermi energy and Fermi surface

The Fermi surface, according to the independent particle approach, is the surface in **k**-space that separates unoccupied from occupied states when the system is at 0 °K. The most general method of determining the surface of magnesium, once the function $E(\mathbf{k})$ is known, consists of determining the surfaces $E(\mathbf{k}) = E_0$ and calculating the value $E_0 = E_F$ for which the volume in **k**-space occupied by the states $E(\mathbf{k}) \leqslant E_F$ is equal to twice the volume of the Brillouin zone. This method involves the calculation of $E(\mathbf{k})$ at many points of the zone and consequently it requires a long running time in the computer. However, since the accuracy of the present calculation is of the order 0·03 Ry, it is possible to determine the Fermi energy E_F by some approximate methods which give results within the specified error. The information concerning the value of E_F in magnesium was obtained by comparison with the free electron model and checked against experimental evidence from X-ray emission spectra and anomalous skin effect data.

In the free-electron model it is assumed that there is no net periodic potential due to the lattice; this only gives rise to the existence of the Brillouin zone and neutralizes the effect of the cloud of negative charge due to the conduction electrons. The single particle energies are then expressed by

$$E(\mathbf{k}) = k^2 + V_{ce}, \tag{6·1}$$

where V_{ce} is the correlation and exchange contribution. We take account of this by means of the Bohm & Pines approximation as given by (2·14) and table 5. The surfaces of constant energy in this model are spheres $|\mathbf{k}| =$ constant. These spheres must be rearranged into more complicated surfaces when they overlap into a Brillouin zone other than the first (Harrison 1960). For

$$|\mathbf{k}| = 0{\cdot}7274 \tag{6·2}$$

the volume of the corresponding sphere is equal to twice the volume of the Brillouin zone, i.e. the sphere of this radius is the Fermi surface. Inserting this value of $|\mathbf{k}|$ into (6·1) and measuring energies from the bottom of the band $\mathbf{k} = 0$, we obtain the value of the Fermi energy for the free electron model,

$$E_{\mathrm{F.}}^{\mathrm{free}} = 0{\cdot}688\ \mathrm{Ry}. \tag{6·3}$$

Comparison of $E(\mathbf{k})$ as calculated with the corresponding curves derived from (6·1) shows an apparent similarity between both; the calculated band structure, except for the splitting of some degeneracies, looks in general like the free-electron model and the effective mass over the conduction band as a whole is very close to the free-electron mass. Consequently the Fermi energy must be very near the free-electron value (6·3). We have compared the values of the computed $E(\mathbf{k})$ at the symmetry points with those given by the free-electron model, and, as an average, the former are about 0·01 Ry smaller than the latter. This would suggest that the Fermi level must be decreased by about the same amount, giving

$$E_{\mathrm{F.}} \simeq 0{\cdot}68\ \mathrm{Ry}. \tag{6·4}$$

We have confirmed the accuracy of this value by using experimental information obtained from the X-ray emission spectra. Skinner (1939) and Cady & Tomboulian (1941) have measured the magnesium L III emission spectrum. This corresponds to transitions between the conduction band and the $2p$ core level. The total width of the spectrum should theoretically give the width of the conduction band, from the bottom up to the Fermi level. But

in fact the actual spectra present a long tail on the low-energy side owing to emission of Auger electrons. It would be necessary then to subtract this effect by means of a suitable extrapolation, but the results would not be reliable due to the doubts existing in the choice of the extrapolating method. Moreover, it is known that the single-particle approach is not valid for states far from the Fermi surface and so the low energy part of the spectrum cannot be fully explained in terms of that model.

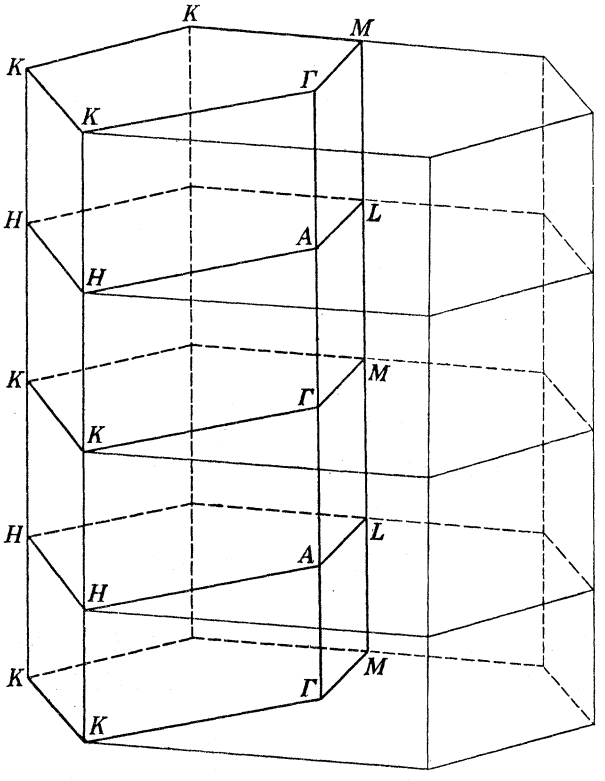

FIGURE 3. The double zone in **k**-space chosen to represent the Fermi surface.

The L III spectrum gives information only about the *s*- or *d*-like electrons. The appearance in the experimental curve of a high and narrow peak on the high-energy side suggests the existence of pockets of electrons with the proper symmetry in the third and fourth zone. These can easily be identified with the electrons near Γ_4^- and K_5, which have the desired symmetry. The extrapolation of the peak gives a total width of about 0·08 Ry. Consequently the Fermi level must be about 0·08 Ry over the value of the energy at Γ_4^-, which gives approximately the same value (6·4) obtained by comparison with the free-electron model.

Finally, measurements of the area of the Fermi surface in magnesium by means of anomalous skin effect measurements (Fawcett 1961) show that fairly good agreement between theory and experiment is achieved if the Fermi level is taken to be about 0·68 Ry. We may conclude then that the value obtained by comparison with the free-electron model gives the Fermi energy within the accuracy obtained for the band energy values.

As mentioned in §4, to describe the Fermi surface we choose a zone in **k**-space equal to two Brillouin zones making contact with each other through their hexagonal faces; this is shown in figure 3. Since the calculated band structure is similar to that resulting from the free-electron model, the Fermi surfaces in both cases must necessarily be alike. The free

electron Fermi surface for a divalent metal in the h.c.p. structure of perfect packing ratio has been published by Harrison (1960). The surface resulting from our calculation differs from it, apart from a change in the c/a ratio and the relative size of each piece, mainly in the smoothing out of the sharp edges caused by the intersection of different parts of the rearranged sphere.

If the conduction electrons in magnesium were tightly bound, the first double zone would be completely full while the third and fourth would be empty. Since this is not the case, the first double zone has a region not occupied by electrons; we call this the region of holes or the 'monster'. On the other hand, some electrons occupy several bits of the third and fourth zone which are called the 'pockets' of electrons. It is evident that the volume of the 'monster' equals the total volume of the pockets of electrons.

In the calculated structure there are nine pockets of three different kinds:

(a) One pocket of electrons around Γ. This corresponds to the Γ_4^- level and the electrons are mainly s-like. The pocket has symmetry 6/mmm around Γ and its approximate shape is that of an oblate spheroid. The approximate radii from Γ to the surface are

$$\left.\begin{aligned} r_{00,1} &= 0{\cdot}058 \quad \Gamma \to A \\ r_{10,0} &= 0{\cdot}255 \quad \Gamma \to M \\ r_{11,0} &= 0{\cdot}253 \quad \Gamma \to K \end{aligned}\right\} \text{ third zone,}$$

where the indices refer to the reciprocal lattice. These values are only approximate and we can estimate the error to be about 20 %. For comparison the size of the Brillouin zone is given in table 3.

(b) Two identical pockets around K. They correspond to one of the branches of the double level K_5. They have symmetry $\bar{6}$ around K. Each pocket looks like a cigar of triangle-like section. The radii from K are

$$\left.\begin{aligned} r_{00,1} &= 0{\cdot}277 \quad K \to H \\ r_{11,0} &= 0{\cdot}073 \quad K \to \Gamma \\ r_{11,0} &= 0{\cdot}044 \quad K \to M \end{aligned}\right\} \text{ third zone,}$$

within a 20 % accuracy.

(c) Six identical pockets around L. They correspond to the second L_1 level. Their symmetry around L is mm^2 and their shape may resemble that of a butter bean. The radii from L, within an accuracy of about 50 %, are

$$\begin{aligned} r_{00,1} &= 0{\cdot}029 \quad L \to M \quad \text{fourth zone,} \\ r_{00,1} &= 0{\cdot}050 \quad L \to M \quad \text{third zone,} \\ \left.\begin{aligned} r_{10,0} &= 0{\cdot}022 \quad L \to A \\ r_{12,0} &= 0{\cdot}043 \quad L \to H \end{aligned}\right\} &\text{ third and fourth zones.} \end{aligned}$$

The various pockets of electrons described above are shown in figure 4, where 5/12 of the double Brillouin zone has been represented in order to exhibit sections of the surface by planes ΓAML and ΓAKH.

In contrast to the electrons of the third and fourth zone, the holes in the first and second zone are in a single, multiply-connected region of symmetry 6/mmm around Γ which makes

contact with the zone boundaries near the twelve H points. This 'monster' can be qualitatively described as consisting of:

(a) A hexagonal shaped ring placed in the plane ΓKM. The radii from Γ are approximately

10, 0 direction	$\Gamma \rightarrow M$	internal radius 0·415, external radius 0·452;
11, 0 direction	$\Gamma \rightarrow K$	internal radius 0·405, external radius 0·606.

The total height of the ring is about 0·125.

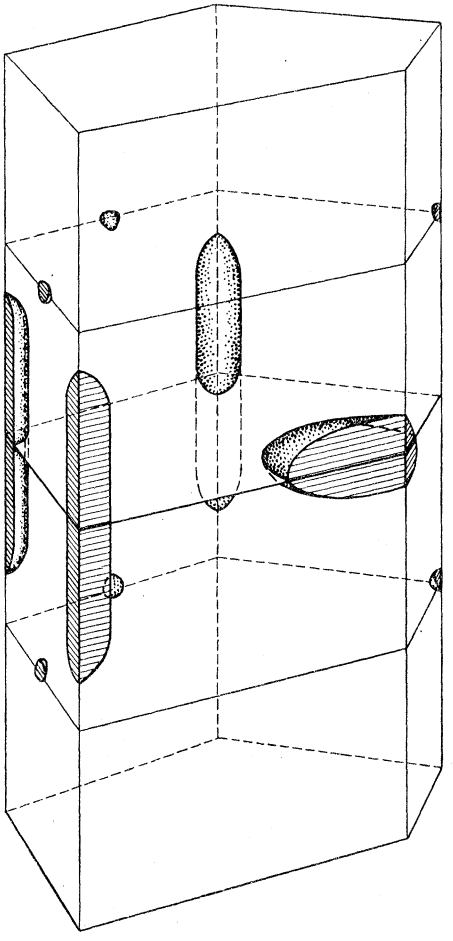

FIGURE 4. The Fermi surface in the third and fourth zone showing sections of the various pockets of electrons. The part of the zone shown here is that drawn in heavy lines in figure 3.

(b) Twelve tentacles coming from the top and bottom of the ring and making contacts with the zone boundaries in very small regions near the H points of the double Brillouin zone. The approximate dimensions of the areas of contact, measuring from H, are

$r_{00,1} = 0{\cdot}044$	$H \rightarrow K$	first zone,
$r_{00,1} = 0{\cdot}044$	$H \rightarrow K$	second zone,
$r_{11,0} = 0{\cdot}012$	$H \rightarrow L$	first and second zones.

PHILOSOPHICAL TRANSACTIONS OF THE ROYAL SOCIETY A MATHEMATICAL, PHYSICAL & ENGINEERING SCIENCES

The 'monster' is shown in figure 5. Figure 6 shows sections of the hole surface with various planes (00, 1) at different heights; we have taken a repeated zone scheme in order to show how three tentacles belonging to three different zones converge to the common H point where they join each other.

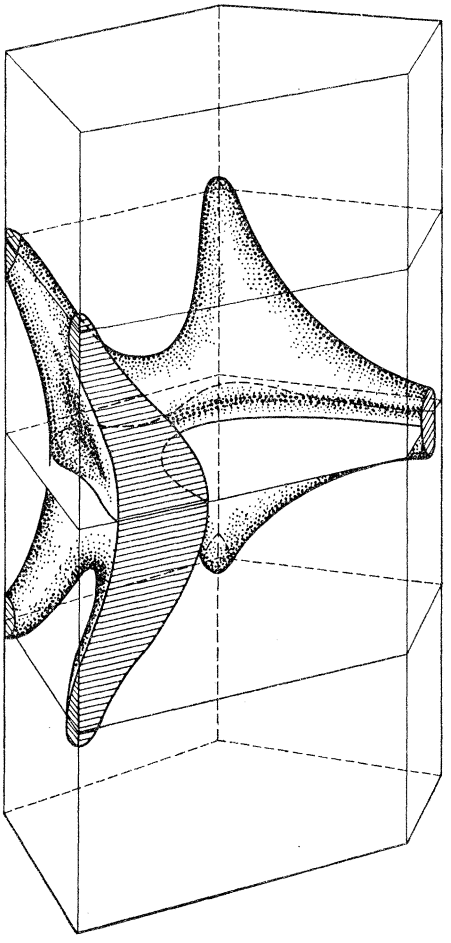

FIGURE 5. The Fermi surface of magnesium in the part of the first and second zone shown by heavy lines in figure 3.

It is interesting to note that due to the presence of the double level P_3 along HK and to the existence of an accidental degeneracy along ΓK of the two levels T_1 and T_4 near the Fermi level the cigar-like pockets and the monster run very near each other in the ΓKAH planes and it is very likely that they even have a point of contact in that plane, near the ΓKM plane, giving rise to a kink in both parts of the Fermi surface. The implication of these nearly degenerate levels has been discussed by Cohen & Falicov (1961) in connexion of electronic transitions between different pieces of the Fermi surface in the presence of high magnetic fields.

Another property of the Fermi surface of considerable interest is the existence of the so-called 'open orbits', i.e. sections of the surface with planes giving rise to intersection lines which do not close themselves. These open orbits play a fundamental role in determining the galvanomagnetic properties of the metal (Lifshitz, Azbel & Kaganov 1956; Lifshitz & Peschanskii 1958).

From our description of the Fermi surface it is evident that only the 'monster' may give rise to open orbits, the electron pieces being closed surfaces. If spin-orbit coupling is neglected, the open orbits can only have a general direction in the basal plane. A careful study of the surface shows that they can only be obtained by sections with planes $(11, l)$ and their general direction is $[10, 0]$.

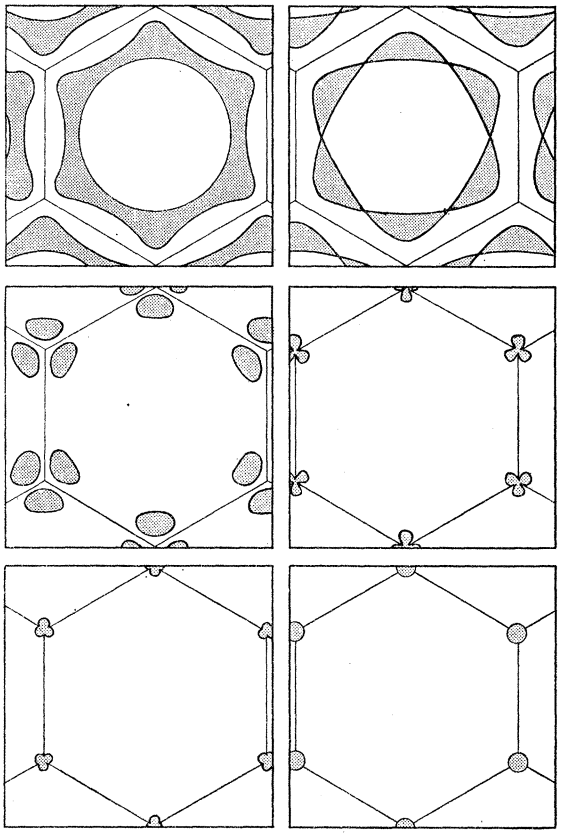

FIGURE 6. Sections of the 'monster' in the repeated zone scheme with planes (00, 1) at various heights.

An estimate based on the given dimensions of the surface gives open orbits for planes $(11, l)$ whose normals form an angle with the c-axis greater than 71° and smaller than 81°. However, this estimate is very sensitive to the dimensions of the surface. The given range of angles increases if

(a) the areas of contact of the monster with the zone boundaries increase,

(b) the height of the ring increases, or

(c) the internal radius of the ring decreases.

If the Fermi level is displaced slightly upwards, these three factors all combine to reduce greatly the range of angles giving open orbits. In the extreme cases of either the H_2 energy level or the degenerate level of the ΓM line being below the Fermi energy, the single sheet of the monster collapses into several unconnected sheets from which no open orbits could be obtained. This is not expected to be the actual case, since experimental evidence indicates the existence of a single, multiply-connected, sheet of surface due to the holes (Gordon *et al.* 1960).

When spin-orbit coupling is taken into account, the sticking together of the bands in the *ALH* plane is removed and the double-zone scheme ordinarily used in the representation of the Fermi surface is no longer valid. This has practically no consequence in the description of the electron pockets, but changes fundamentally the topology of the 'monster'. The small pockets of holes in the first zone must be removed from the 'monster', and the latter then repeats itself along the c axis as shown in figure 7. The new hole surface shows again the same open orbits described above, but another kind of open orbits appear in addition. These have the general direction [00, 1] and are obtained by section with any plane $(hk, 0)$ parallel to the c axis.

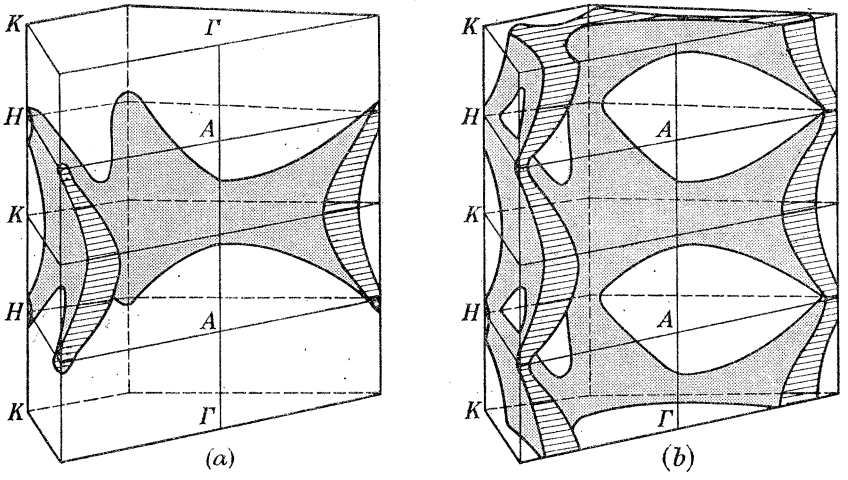

FIGURE 7. The change in the connectivity properties of the 'monster' due to spin-orbit coupling (*a*) the 'without spin' case; (*b*) the 'monster' when spin-orbit coupling is taken into account.

The author is deeply indebted to Dr V. Heine for suggesting this problem and for his constant and illuminating supervision. He wishes to thank Professor M. H. Cohen, Dr J. G. Collins, Dr E. Fawcett, Dr J. C. Phillips, Professor A. B. Pippard, F.R.S., Dr M. G. Priestley, Dr D. Shoenberg, F.R.S., and Dr J. M. Ziman for several stimulating discussions. He is also grateful to the University of Cambridge Mathematical Laboratory for permission to use the computer and to its staff for the advice given in programming, to the University of Buenos Aires for the grant of a post-graduate scholarship, and to the Institute for the Study of Metals, University of Chicago, where this work was completed.

REFERENCES

Altmann, S. L. 1958 *Proc. Roy Soc.* A, **244**, 141.
Antoncik, E. & Triflaj, M. 1952 *Czek. J. Phys.* **1**, 97.
Bernal, M. L. M. & Boys, S. F. 1952 *Phil. Trans.* A, **245**, 139.
Biermann, L. & Trefftz, E. 1949 *Z. Astrophys.* **26**, 123.
Bouckaert, L. P. Smoluchowski, R. & Wigner, E. 1936 *Phys. Rev.* **50**, 58.
Cady, W. M. & Tomboulian, D. H. 1941 *Phys. Rev.* **59**, 381.
Callaway, J. 1958 *Solid state physics*, **7**, 100. New York: Academic Press.
Cohen, M. H. & Falicov, L. M. 1960 *Phys. Rev. Lett.* **5**, 544.
Cohen, M. H. & Falicov, L. M. 1961 *Phys. Rev. Lett.* **6**, 231.

PHILOSOPHICAL TRANSACTIONS OF THE ROYAL SOCIETY A MATHEMATICAL, PHYSICAL & ENGINEERING SCIENCES

Cohen, M. H. & Heine, V. 1958 *Advanc. Phys.* **7**, 395.
Elliott, R. J. 1954 *Phys. Rev.* **96**, 280.
Falicov, L. M. & Heine, V. 1961 *Advanc. Phys.* **10**, 57.
Fawcett, E. 1961 *J. Phys. Chem. Solids*, **4**, 320.
Fletcher, J. G. & Larson, D. C. 1958 *Phys. Rev.* **111**, 455.
Gell-Mann, M. & Brueckner, K. A. 1957 *Phys. Rev.* **106**, 364.
Gordon, W. L., Joseph, A. S. & Eck, T. G. 1960 *The Fermi surface*, p. 84. New York: Wiley.
Harrison, W. A. 1960 *Phys. Rev.* **118**, 1190.
Hartree, D. R. 1957 *The calculation of atomic structures.* New York: Wiley.
Hartree, D. R. & Hartree, W. 1948 *Proc. Roy. Soc.* A, **193**, 299.
Heine, V. 1957 *Proc. Roy. Soc.* A, **240**, 340, 361.
Herman, F. 1955 *Proc. Inst. Radio Engrs., N.Y.*, **43**, 1703.
Herman, F. 1958 *Rev. Mod. Phys.* **30**, 102.
Herring, C. 1937*a* *Phys. Rev.* **52**, 361.
Herring, C. 1937 *b* *Phys. Rev.* **52**, 365.
Herring, C. 1942 *J. Franklin Inst.* **233**, 525.
Hubbard, J. 1958 *Proc. Roy. Soc.* A, **244**, 199.
Jacque–Yost, W. 1940 *Phys. Rev.* **58**, 559.
Kittel, C. 1956 *Introduction to solid state physics.* New York: Wiley.
Lifshitz, I. M., Azbel, M. Ia & Kaganov, M. I. 1956 *J. exp. theor. phys.* **31**, 63 [translation *Soviet Physics*, **31** (4), 41].
Lifshitz, I. M. & Peschanskii, V. G. 1958 *J. exp. theor. phys.* **35**, 1251 [translation *Soviet Physics*, **35**, (8), 875].
Nozières, P. & Pines, D. 1958 *Phys. Rev.* **111**, 442.
Pines, D. 1955 *Solid state physics*, **1**, 368. New York: Academic Press.
Priestley, M. G. To be published.
Reitz, J. R. 1955 *Solid state physics*, **1**, 2. New York: Academic Press.
Skinner, H. W. B. 1940 *Phil Trans.* A, **239**, 95.
Shoenberg, D. 1960 *The Fermi surface*, p. 74. New York: Wiley.
Woodruff, T. O. 1957 *Solid state physics*, **4**, 367. New York: Academic Press.

PHILOSOPHICAL TRANSACTIONS OF THE ROYAL SOCIETY A MATHEMATICAL, PHYSICAL & ENGINEERING SCIENCES